

Nonlinear oscillations of gas bubbles in liquids: transient solutions and the connection between subharmonic signal and cavitation

Andrea Prosperetti*

California Institute of Technology, Pasadena, California 91125

(Received 6 August 1974; revised 4 December 1974)

The transient nonlinear oscillations of a spherical gas bubble in an incompressible, viscous liquid subject to the action of a sound field are investigated by means of an asymptotic method. Approximate analytical solutions are presented for the frequency regions of the fundamental resonance, the first and second subharmonic, and the first and second harmonic. Based on the results of this investigation, a new hypothesis to explain the connection between subharmonic signal and cavitation is put forward. It is suggested that bubbles emitting the subharmonic signal act primarily as monitors of cavitation events, and are smaller than resonance size. Finally, the free oscillations of the bubble are briefly considered.

Subject Classification: 25.60; 30.70, 30.75.

LIST OF SYMBOLS

b	dimensionless damping coefficient, Eq. 4
c_i	$0 \leq i \leq 6$, functions of the forcing frequency, Eqs. A1–A7
C	slowly varying amplitude of the resonant component
C_0	steady-state value of the amplitude of the 1/2 order (first) subharmonic component, Eqs. 10a, 11
d_i	$1 \leq i \leq 3$, functions of the forcing frequency, Eqs. A17–A19
g_i	$0 \leq i \leq 6$, functions of the forcing frequency, Eqs. A10–A16
h_i	$1 \leq i \leq 3$, functions of γ and w , Eqs. 25
H	Hamiltonian function for the system of equations determining the slowly varying amplitude and phase, Eqs. 13, 18, 20
n	numerical constant, Table I
p_0	internal pressure of the bubble at equilibrium
p_∞	average value of the ambient pressure
R	radius of the bubble
R_0	value of the radius at equilibrium
R_{\max}	maximum value of the radius in an oscillation
t	dimensional time
u, v	phase-plane coordinates, Eqs. 12
w	Weber number, Eq. 3
x	normalized dimensionless radius, Eq. 2

Greek characters

α_1, α_2	functions of γ and w , Eq. 4
β_1, β_2	functions of the forcing frequency, Eqs. A8, A9
γ	polytropic exponent
Δ	phase of the component of frequency ω in the steady state, Eq. 8
η	amplitude of the sound field relative to p_∞ , Eq. 1
θ	phase of the resonant component, Eqs. 8, 24
λ_1, λ_2	numerical constants, Table I
Λ	logarithmic decrement of the free oscillations, Eq. 28
μ	liquid viscosity
ξ	"effective" dimensionless sound field amplitude, Eq. 4
ρ	liquid density
σ	surface tension of the liquid
τ	dimensionless time, Eq. 2
φ	slowly varying part of the phase of the resonant component, Eq. 8
ω	dimensionless frequency of the sound field, Eq. 3
ω_0	dimensionless natural frequency of the bubble, Eq. 3
ω_{NL}	dimensionless natural frequency of the nonlinear, free oscillations, Eq. 27
Ω	dimensional frequency of the sound field
Ω_0	dimensional natural frequency of the bubble

INTRODUCTION

The highly nonlinear structure of the equations describing the dynamics of a gas bubble in a liquid renders very difficult the investigation of the transient oscillations of the bubble under the action of a sound field. The relevance of such transient oscillations in the phenomena of acoustic cavitation has long been appreciated,¹ but it appears that the only results available in the literature have been obtained by numerical rather than analytical methods.^{1–3,25} In this study we present an approximate analytical investigation of the transient oscillations in the frequency regions of the first and second subharmonic, first and second harmonic, and of the fundamental

resonance. The bubble is assumed to remain spherical and to oscillate nonlinearly in an incompressible, viscous liquid under the action of a sound field whose wavelength is large compared with the bubble radius.

The results presented here illustrate very clearly the great importance of the initial conditions on the motion. In certain cases, a small change in the initial velocity or deformation of the bubble can lead to strikingly different motions. Even the characteristics of the steady-state oscillations are often quite sensitive to this element, a typical example being the presence or absence of a subharmonic component in them. This point has not always been evident to workers in the field, whose

results may sometimes be incomplete and also misleading due to a lack of its discussion.

The effect of initial conditions could also have far-reaching consequences as far as an explanation of the puzzling phenomenon of the connection between subharmonic emission and cavitation⁴⁻⁸ is concerned. A new interpretation of this effect is suggested here, in which the shocks radiated by the collapsing cavities excite a subharmonic emission from bubbles smaller than resonance size.

The last topic considered is that of the free oscillations of gas bubbles. In particular, the lowest-order correction to the oscillation frequency is determined explicitly.

In a previous study closely related to the present one,⁹ the same asymptotic method used here was applied to the steady-state oscillations; there it was shown that the results obtained in this way compared quite favorably with results obtained by numerical integration of the same equation,¹⁰ as long as the amplitude of the oscillation $(R_{\max} - R_0)/R_0$, with R_0 the equilibrium radius, did not exceed ~ 0.3 . The qualitative features of the motion, however, were preserved with surprising accuracy for much larger values of the oscillation amplitude. Although it has not been possible to find in the literature numerical results suitable for comparison with the transient solutions obtained here, it is presumed that the accuracy of the present results would be similar to that found in the steady case.

I. PRELIMINARIES

Under the hypotheses stated in the Introduction, the Rayleigh-Plesset equation of motion for the wall of a spherical bubble of radius $R(t)$ can be written as¹¹

$$R \frac{d^2 R}{dt^2} + \frac{3}{2} \left(\frac{dR}{dt} \right)^2 = \frac{1}{\rho} \left[p_0 \left(\frac{R_0}{R} \right)^{3\gamma} - p_\infty (1 - \eta \cos \Omega t) - \frac{2\sigma}{R} - \frac{4\mu}{R} \frac{dR}{dt} \right]. \quad (1)$$

In this equation p_∞ is the average value of the ambient pressure, on which a sound field of amplitude ηp_∞ and frequency Ω is superimposed. The behavior of the gas contained in the bubble has been approximated by a polytropic relation with polytropic exponent γ , and the equilibrium radius R_0 is related to the constants p_0 , p_∞ by the relation $p_0 - p_\infty = 2\sigma/R_0$. If the conditions are such that thermal and acoustic damping are important, the viscous constant μ can be suitably modified to account in an approximate way for such dissipation mechanisms in the manner indicated in Refs. 9 and 12. These references contain also a discussion of the other approximations involved in Eq. 1.

Let us introduce the following quantities:

$$R = R_0(1 + x), \quad \tau = (p_0/\rho)^{1/2} R_0^{-1} t, \quad (2)$$

$$\omega = (\rho/p_0)^{1/2} R_0 \Omega, \quad \omega_0^2 = 3\gamma - w, \quad w = 2\sigma/R_0 p_0, \quad (3)$$

$$b = 2\mu/R_0(\rho p_0)^{1/2}, \quad \xi = (1 - w)\eta, \quad (4)$$

$$\alpha_1 = \frac{9}{2}\gamma(\gamma + 1) - 2w, \quad \alpha_2 = \frac{1}{2}\gamma(9\gamma^2 + 18\gamma + 11) - 3w.$$

If Eq. 2 is substituted into Eq. 1 and a power series ex-

pansion in powers of x is carried out, one obtains

$$\ddot{x} + \omega_0^2 x = \xi \cos \omega t + \alpha_1 x^2 - \frac{3}{2} \dot{x}^2 - x \xi \cos \omega t - 2b\dot{x} + \frac{3}{2} \dot{x}^2 x - \alpha_2 x^3 + x^2 \xi \cos \omega t + 4bx\dot{x}. \quad (5)$$

Terms of the form $b^i x^j \dot{x}^k \xi^l$, with i, j, k, l nonnegative integers such that $i + j + k + l > 3$, have been dropped. It is evident from this equation that the constant ξ acts as an "effective pressure amplitude" for the oscillations which decreases with the equilibrium radius; the constant ω_0 has the meaning of resonance frequency of the bubble; when it is converted back into dimensional form according to Eq. 3 the well-known result^{13,14}

$$\Omega_0^2 = [3\gamma(p_\infty + 2\sigma/R_0) - 2\sigma/R_0]/\rho R_0^2 \quad (6)$$

is recovered.

To third order in the perturbation Eq. 5 possesses two harmonics $[\omega \sim (1/2)\omega_0$ and $\omega \sim (1/3)\omega_0]$ and two subharmonics ($\omega \sim 2\omega_0$ and $\omega \sim 3\omega_0$) in addition to the fundamental resonance $\omega \sim \omega_0$. In all of these frequency regions except the last one (which will be considered separately in Sec. IV) the solution $x(\tau)$ is found to have a similar form, namely:

$$x(\tau) = C(\tau) \cos \theta + \xi [(\omega^2 - \omega_0^2)^2 + 4b^2 \omega^2]^{-1/2} \cos(\omega t + \Delta) + (c_1 + \lambda_1 c_3 \cos 2\omega t) \xi^2 + (c_5 + c_2 \cos 2\theta) C^2(\tau) + [c_4 \cos(\omega \tau + \theta) + \lambda_2 c_0 \cos(\omega \tau - \theta)] \xi C(\tau), \quad (7)$$

where

$$\Delta = \tan^{-1}[2b\omega/(\omega^2 - \omega_0^2)], \quad (8)$$

$$\theta = n\omega\tau + \varphi(\tau),$$

and the c_i 's, $0 < i < 5$, are functions of ω , γ , and w given by Eqs. A1-A7 of the Appendix. The time-dependent amplitude $C(\tau)$ and phase $\varphi(\tau)$ of the resonant component will be discussed separately for each resonant frequency region below.

The transient solutions of Eq. 7 in the resonant frequency regions have been determined with the aid of the Bogoliubov-Krylov method of averaging.^{15,16} A brief outline of the procedure is contained in Ref. 9, and additional details on the computations and results can be found in Ref. 12. The Bogoliubov-Krylov method can also be applied to obtain solutions in frequency regions other than those containing resonances. Since however the amplitude of oscillation in these regions is small, their interest is rather limited and they will not be considered.

TABLE I. Values of the constants appearing in Eq. 7 in the different frequency regions.

	n	λ_1	λ_2
1st subharmonic region	1/2	1	0
2nd subharmonic region	1/3	1	1
1st harmonic region	2	0	1
2nd harmonic region	3	1	1
Intermediate regions	...	1	...

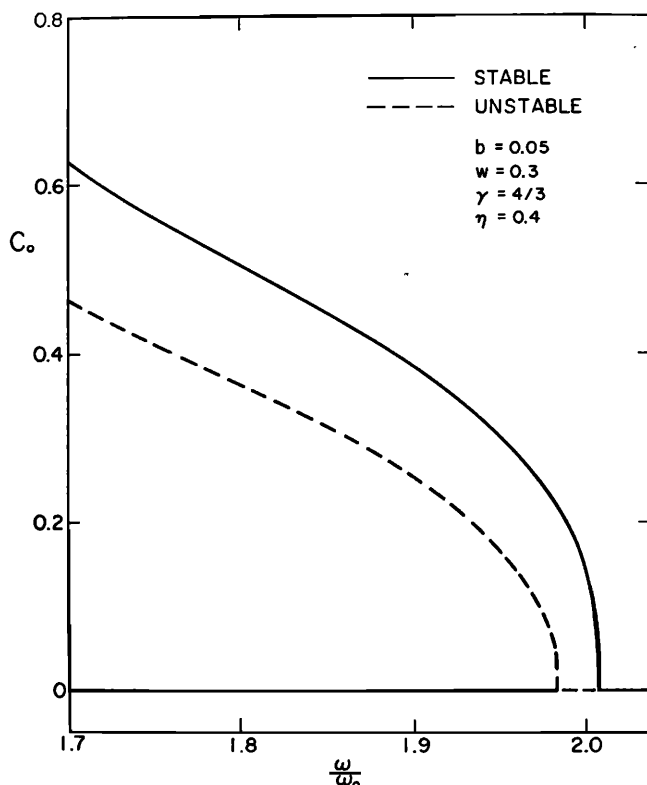


FIG. 1. Amplitude of the steady-state subharmonic component as a function of the ratio between the impressed frequency ω and the natural frequency of the bubble ω_0 in a typical case.

II. THE FIRST SUBHARMONIC

The equations determining the amplitude and phase of the resonant component in the region of the first (or 1/2-order) subharmonic are

$$-\omega \dot{C} = \omega b C - \beta_1 \xi C \sin 2\varphi + b g_4 \xi C \cos 2\varphi, \quad (9a)$$

$$-\omega C \dot{\varphi} = Q_{1/2} C + g_0 C^3 - \beta_1 \xi C \cos 2\varphi - b g_4 \xi C \sin 2\varphi, \quad (9b)$$

where

$$Q_{1/2} = (1/4)\omega^2 - \omega_0^2 - \xi^2 g_1.$$

The critical points C_0 and φ_0 of this system (i.e., the values of C and φ that satisfy Eqs. 9 with vanishing left-hand sides) correspond to the steady-state oscillations and are given by

$$C_0 = g_0^{-1/2} [-Q_{1/2} \pm (\beta_1^2 \xi^2 - b^2 \omega^2)^{1/2}]^{1/2}, \quad (10a)$$

$$\tan 2\varphi_0 = b \frac{\omega \beta_1 + g_4 (Q_{1/2} + g_0 C_0^2)}{\beta_1 (Q_{1/2} + g_0 C_0^2)}, \quad (10b)$$

and

$$C_0 = 0, \quad \varphi_0 \text{ arbitrary.} \quad (11)$$

A detailed analysis of these steady-state oscillations and a discussion of the subharmonic threshold obtainable from Eq. 10a are contained in Refs. 9 and 12. Suffices here to say that of the two branches of Eq. 10a the one with the plus sign corresponds to a stable critical point (stable focus), and the other one to an unstable one (saddle point); two values of φ_0 differing by π are associated with each one of these values of C_0 . The third critical point $C_0 = 0$ is stable (stable focus) or unstable (saddle

point) depending on the values of ω/ω_0 and ξ . The interval of instability contains the point $\omega/\omega_0 = 2$ and becomes wider with increasing ξ . A representative example of the response curves determined by Eqs. 10a and 11 is shown in Fig. 1. It can be seen here that there exists a broad frequency interval in which a subharmonic component may or may not be present in the steady-state solutions depending on the initial conditions of the motion, as will now be discussed.¹⁷

The transient solutions are most easily studied in terms of the new variables

$$u = C \cos \varphi, \quad v = C \sin \varphi \quad (12)$$

in the phase plane of the system. The discussion is also facilitated by considering the undamped ($b = 0$) case first, which preserves the essential structure of the solutions. In this case the system in question is Hamiltonian, with a Hamiltonian function given by

$$H[C, \varphi] = \frac{1}{4} g_0 C^4 + \frac{1}{2} Q_{1/2} C^2 - \frac{1}{2} \beta_1 \xi C^2 \cos 2\varphi, \\ = \frac{1}{4} g_0 (u^2 + v^2)^2 + \frac{1}{2} Q_{1/2} (u^2 + v^2) - \frac{1}{2} \beta_1 \xi (u^2 - v^2). \quad (13)$$

Since Eqs. 9 can now be written as

$$\omega C \dot{C} = \frac{\partial H}{\partial \varphi}, \quad \omega C \dot{\varphi} = -\frac{\partial H}{\partial C}, \quad (14)$$

it is readily verified that $dH/d\tau = 0$, so that the curves

$$H[C, \varphi] = \text{constant} = H[C(\tau = 0), \varphi(\tau = 0)] \quad (15)$$

are the unsteady, periodic solutions of Eqs. 9. It should be remarked that this periodicity affects the oscillations of the bubble only as an amplitude modulation, and is therefore of a longer period than the sound field. The system of curves (orbits) determined by Eq. 15 in the (u, v) plane is shown in Fig. 2 for the case $\omega/\omega_0 = 1.8$, $w = 0.2$, $\eta = 0.4$, $\gamma = 1.33$. These values of the parameters correspond to a situation in which the subharmonic component may or may not be present in the steady oscillations. The critical points (now on the coordinate axes, the stable ones on the abscissa and the unstable ones on the ordinate axis) are indicated by large dots, and the numbers labeling the orbits denote the period of modulation in units of $\omega\tau$. The orbits labeled ∞_1 , ∞_2 are the two separatrices passing through the unstable critical points; the inner one encircles the origin, the outer all the stable critical points. It will be noticed that for not too large values of H the orbits are essentially of two kinds, those encircling either one of the two nonzero foci ("subharmonic" orbits) and those encircling the origin ("harmonic" orbits).¹⁸ The full oscillation according to Eq. 7 for the case of the orbit of period 86 $\omega\tau$ is shown in Fig. 3.

When damping is introduced it is no longer possible to find a closed-form solution of the system 9, which however can readily be integrated numerically. Essentially one finds that the "harmonic" orbits spiral into the origin, while the "subharmonic" ones spiral into the other stable singular points (Fig. 4). In the first case the steady-state oscillations will not contain a subharmonic component, which however will be present in the second case. The outer orbits present a variety of behaviors, with the solution spiraling into any one of the

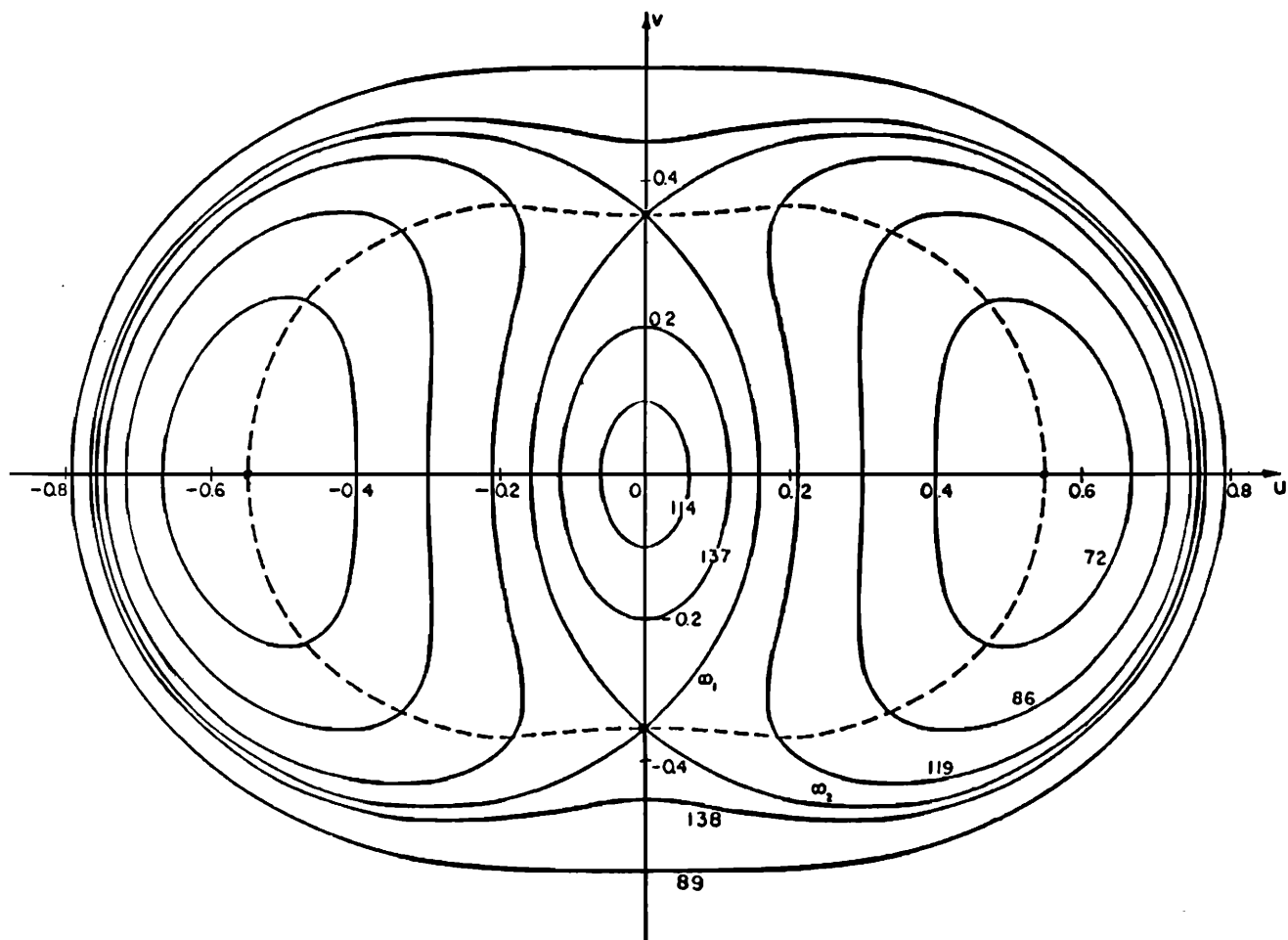


FIG. 2. Solution curves for the system 9 in absence of damping for $\omega/\omega_0=1.8$, $w=0.2$, $\eta=0.4$, $\gamma=1.33$. The numbers along the curves denote their period in units of $\omega\tau$. The two unstable critical points are on the v axis at the intersection of the separatrices, the two nonzero stable ones on the u axis at the intersection with the dashed curve. The latter marks the locus $dH/d\tau=0$ in the presence of damping.

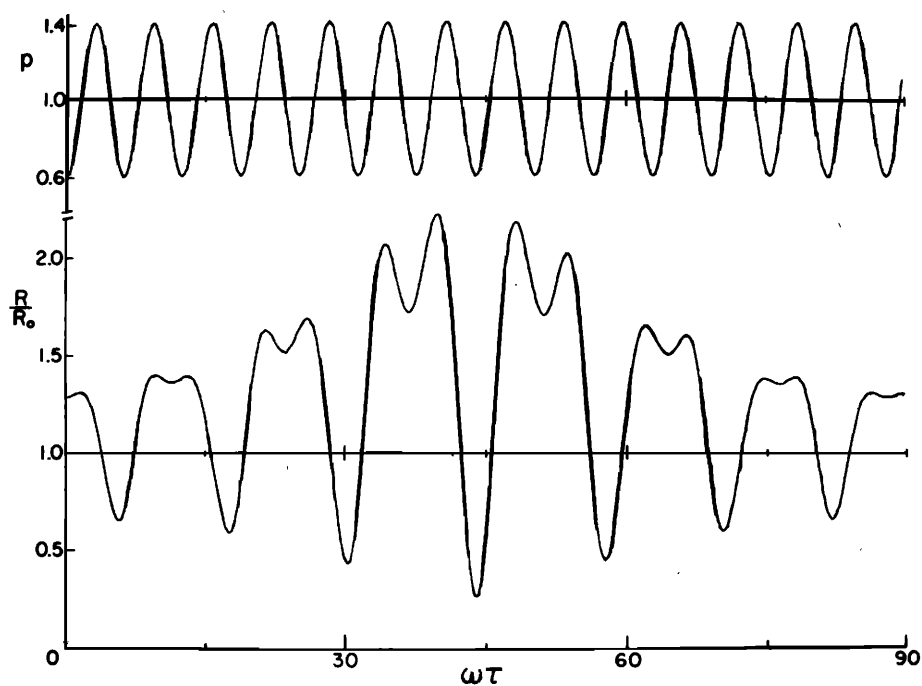


FIG. 3. Modulated subharmonic bubble oscillations as determined by Eq. 7. The modulated amplitude and phase correspond to the orbit of period $86\omega\tau$ in Fig. 2.

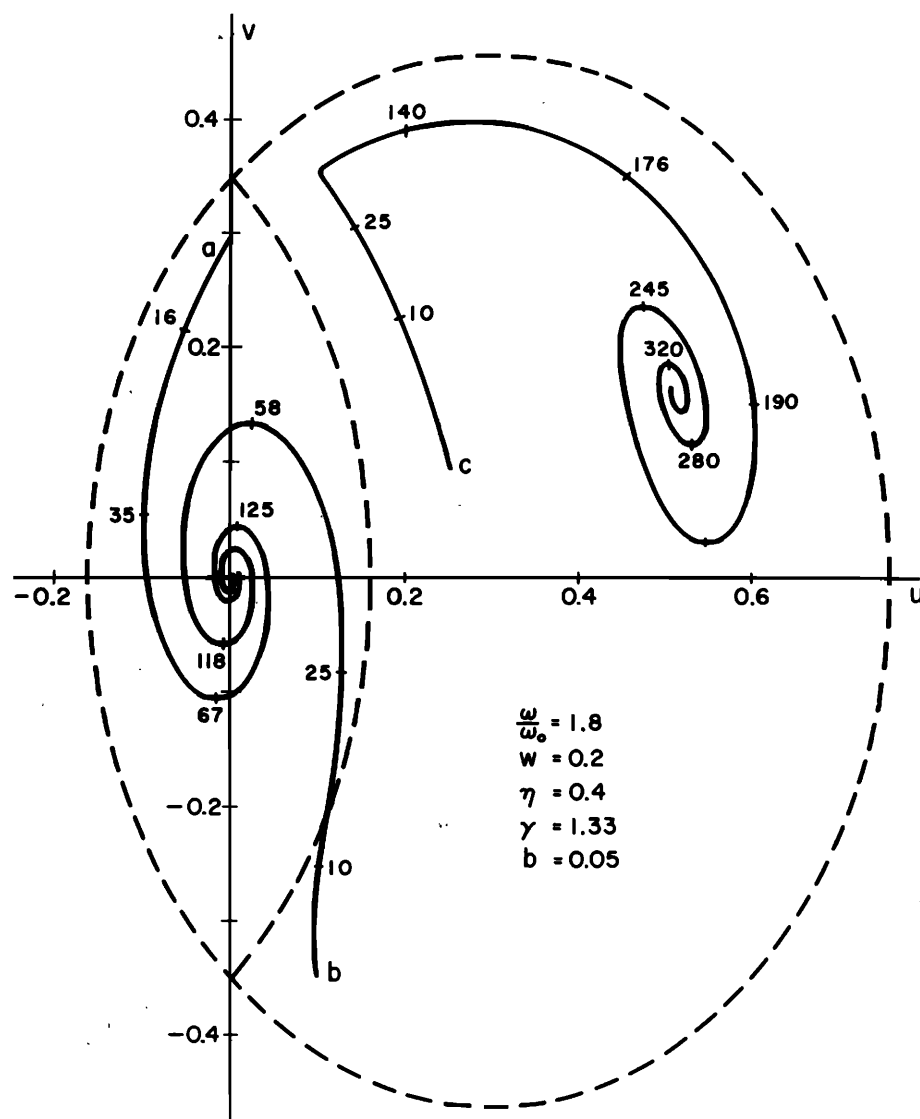


FIG. 4. Three examples of solution curves of the system 9 with damping. The dashed curves are the inner and the right half of the outer separatrix for the undamped case (Fig. 2). The numbers along the curves denote time since the beginning of the motion in units of $\omega\tau$.

three stable foci (Fig. 5). The phase plane is thus divided up into "domains of attraction" of the three singular points, in the way schematically indicated in Fig. 6.

The radius-versus-time curves corresponding to the trajectories labeled by b and c in Fig. 4 are shown in Figs. 7 and 8. It will be noticed that even if the initial amplitude in Fig. 7 is larger than that in Fig. 8, there is no subharmonic component in the steady oscillations in the first case. In Fig. 8 the slowness of the amplitude variations for $30 < \omega\tau < 120$ (corresponding to the vicinity of the "kink" in curve c of Fig. 4) emphasizes once again the difficulty of ascertaining whether a solution obtained by numerical integration of the Rayleigh-Plesset equation corresponds indeed to steady oscillations. It may be noticed that the results presented in this study are potentially useful when an accurate numerical solution is sought, since they allow one to obtain good estimates of the relaxation times of the system, and of the location of the singular points. The time required for convergence to a steady-state solution, for instance, can be significantly reduced by choosing initial conditions in the vicinity of the appropriate singular point.

The phase-plane structure illustrated above remains qualitatively the same in the entire frequency region in which both subharmonic and subharmonic-free steady oscillations are possible. The domain of attraction of the origin, however, gets larger as ω/ω_0 is decreased away from $\omega/\omega_0 = 2$, or as the pressure amplitude η is lowered. This implies that more and more violent perturbations of the subharmonic-free oscillations that the bubble would normally exhibit at these frequencies are required to excite the subharmonic component.

At the value of ω/ω_0 at which the solution $C_0 = 0$ becomes unstable, the inner separatrix disappears and the outer one assumes the shape of the symbol ∞ .¹⁹ Finally, in the region of instability of $C_0 = 0$, the lines $H = \text{constant}$ encircle either one or both the remaining stable foci, and in the presence of damping all solutions spiral into one of them as $\tau \rightarrow \infty$.

III. THE CONNECTION BETWEEN SUBHARMONIC SIGNAL AND ACOUSTIC CAVITATION

The sudden appearance of a strong signal at half the excitation frequency in a liquid at the onset of acoustic

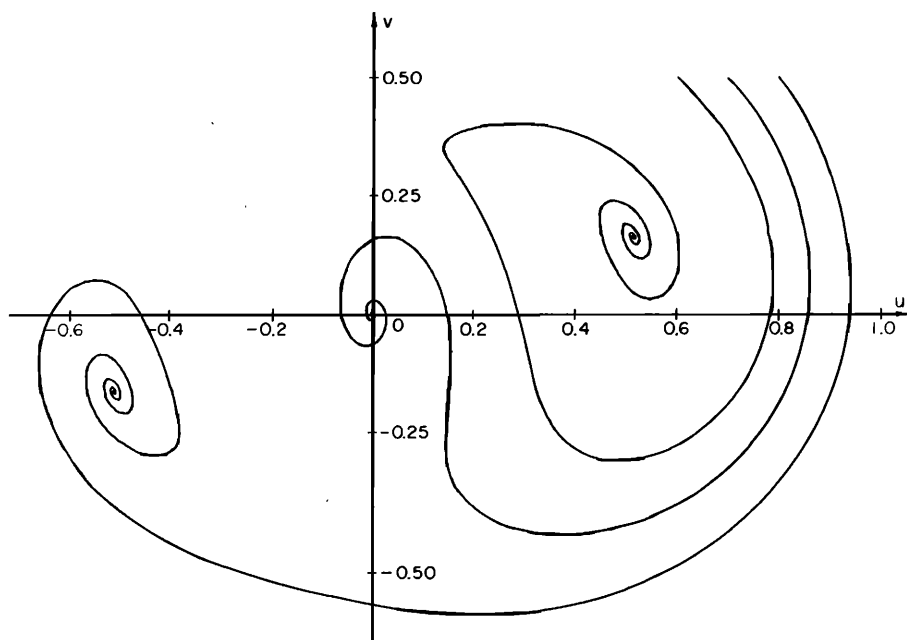


FIG. 5. Three examples of solution curves of the system 9 with damping. All the initial conditions lie outside the outer separatrix. The values of the parameters are the same as in Fig. 4.

cavitation was first observed by Esche in 1952,⁴ and has since then been confirmed by many workers.⁵⁻⁸ It appears to be now established that this signal is connected in some as yet unexplained way with the presence of bubbles in the liquid, although other less important mechanisms may contribute to it (see, e.g., Ref. 8 for a short summary and discussion). That the presence of bubbles of such radii that they resonate at the subharmonic frequency can result in a strong signal at half the frequency of the driving sound field has found further support in the results obtained by Neppiras.^{7,8} To explain the coincidence between the subharmonic signal and the onset of cavitation, he conjectures that the subharmonically oscillating bubbles (which may form in the liquid because of rectified diffusion) become unstable and collapse. This explanation, however, fails to account for

the following features of the phenomenon:

(1) Experiments with single bubbles show that they can oscillate at the subharmonic frequency for long periods of time without evolving into transient cavities.^{7,8} Similarly, in experiments with gassy liquids the subharmonic signal is present without any appreciable white noise.⁶

(2) If bubbles grow from microscopic size by rectified diffusion, they would reach a radius such that their natural frequency is *equal* to that of the sound field long before they would be in the subharmonic size range. Indeed, as Eq. 6 shows, if surface tension is neglected the two radii would differ by a factor of two. It is therefore hard to understand why the instability manifests itself in the subharmonic oscillations rather than in the

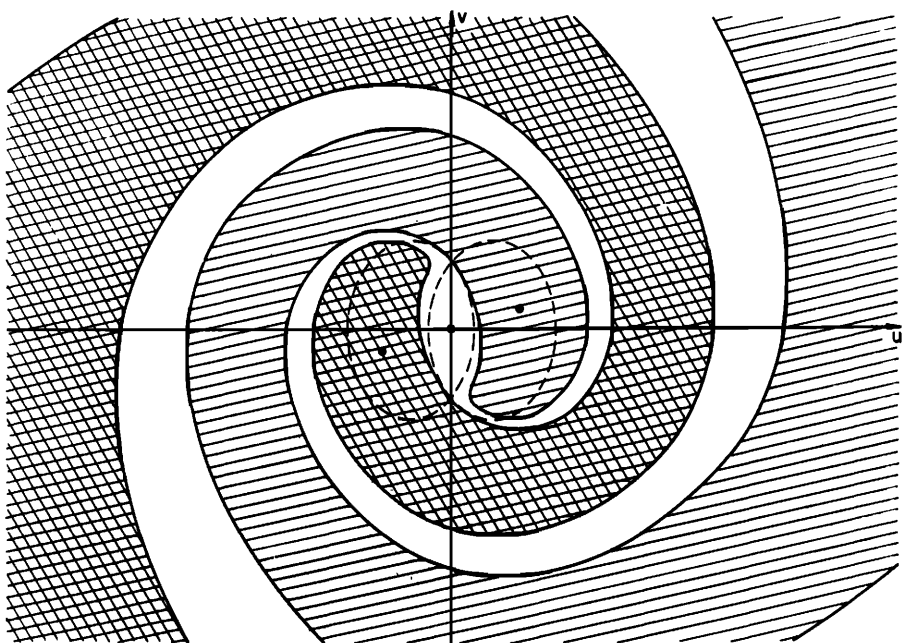


FIG. 6. Qualitative structure of the "domains of attraction" of the three stable singular points (large dots) in the presence of damping. The dashed lines are the separatrices for the undamped case.

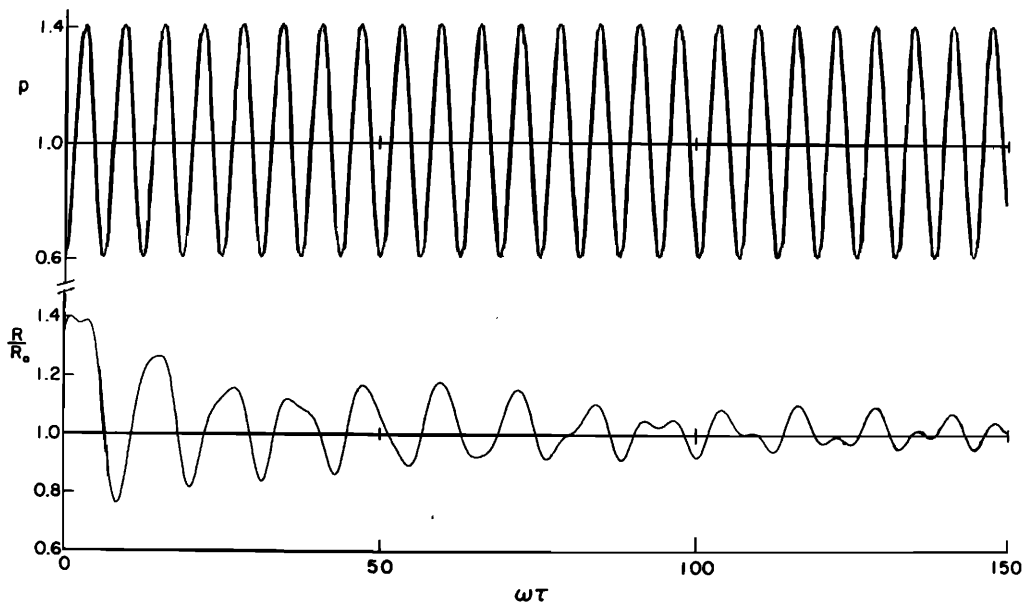


FIG. 7. Modulated bubble oscillations corresponding to the curve *b* of Fig. 4. The steady-state oscillations (not shown) will not contain a subharmonic component.

resonant ones, which are much more violent.

(3) At a sound frequency of a few tens of kilohertz, a bubble resonating at the subharmonic frequency would have a radius of the order of 10^{-1} cm. Such relatively large bubbles have not always been observed in the experiments in which the connection between subharmonic emission and onset of cavitation has been established.¹⁰

In a recent paper Eller²⁰ argues in favor of Neppiras's hypothesis and shows by numerical integration of the Rayleigh-Plesset equation that subharmonic oscillations are possible over a very wide range, for $1 \lesssim \omega/\omega_0 \lesssim 2$. The fact that this mode of oscillation over such a large range has not been reported in the extensive investiga-

tion conducted by Lauterhorn,¹⁰ raises the possibility that one is faced with a very strong effect of the initial conditions of the motion, which unfortunately Eller does not discuss.²¹ Indeed, Eller's results for ω/ω_0 much below 2 correspond to such large amplitude oscillations, that they may demand totally unrealizable initial conditions, such as extremely large initial wall velocities, even greater than those corresponding to resonant oscillations. In addition, Eller's argument is also subject to the criticism expressed in point (2) above.

Another recent result reported by Lauterborn¹⁰ may be relevant for the explanation of the phenomenon in question, namely, the fact that a Fourier component of

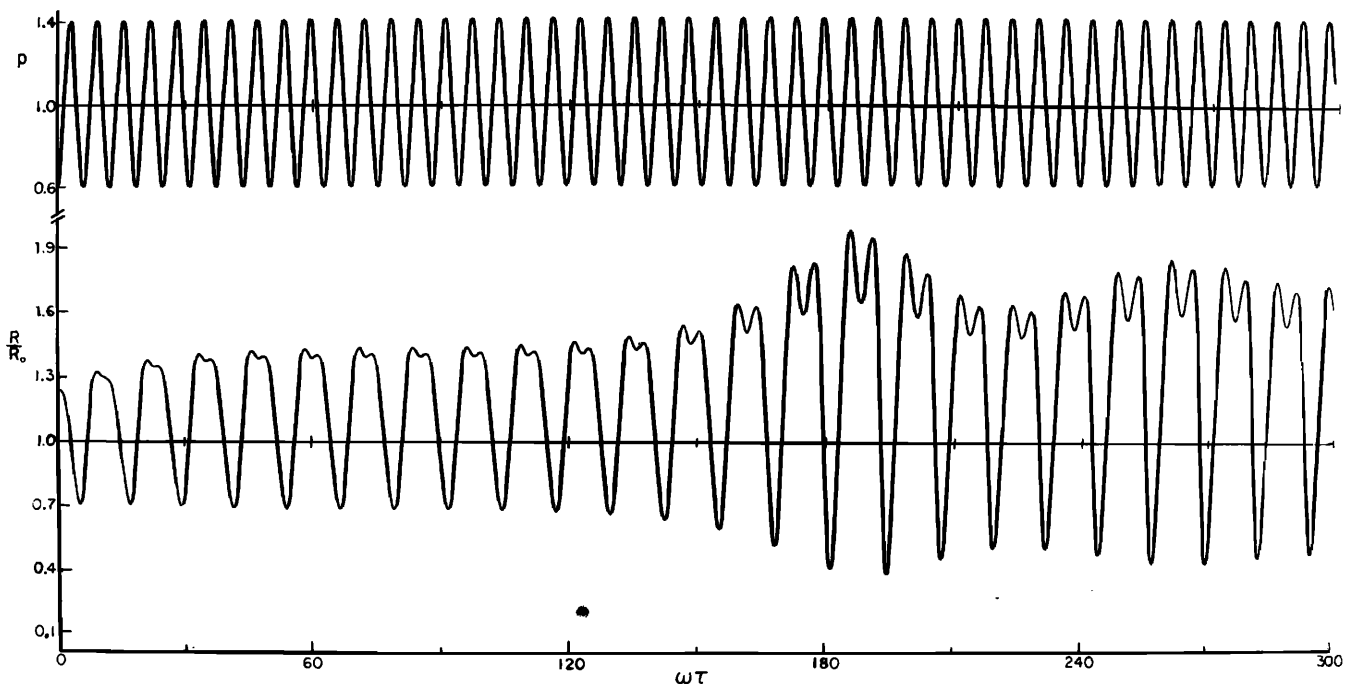


FIG. 8. Modulated bubble oscillations corresponding to the curve *c* of Fig. 4. The steady-state oscillations (not shown) will contain a subharmonic component.

frequency $(1/2)\omega$ is often present in bubbles whose natural frequency satisfies the relation

$$\frac{\omega}{\omega_0} \sim \frac{2}{k}, \quad k=1, 3, 4, \dots \quad (16)$$

For $k=1$ this is the ordinary subharmonic oscillation in the sense discussed in Sec. II. For $k>1$, however, the bubbles satisfying Expression 16 would be smaller than resonance size, so that this theory does not lend itself to the criticisms expressed in points (2) and (3) above.

If this is really the mechanism for the subharmonic emission, however, the connection between its appearance and the onset of cavitation remains to be explained, and also a reason should be given for the absence of a strong subharmonic signal under noncavitating conditions. The analysis of the nonsteady behavior of the subharmonic amplitude presented in Sec. II may serve as a guide towards a satisfactory understanding of these features.

As Fig. 1 shows, and as has been discussed in Ref. 9, the radii of bubbles that would enter *spontaneously* into subharmonic oscillations are rather sharply defined. This can be expected to be true also for the subharmonic emissions from bubbles satisfying Eq. 16, in view of the large number of nonlinear couplings necessary to transfer the energy from the mode ω to the mode $(1/2)\omega$. However, as has been shown above, there exists a much broader frequency domain in which, although the purely harmonic oscillation is stable, a subharmonic oscillation may also be present provided that the initial conditions for the motion lie in a suitable range. In practice this means that, if the purely harmonic motion is sufficiently perturbed, the ensuing oscillations would contain a subharmonic component.

The weak shocks radiated by collapsing cavities in the vicinity of these bubbles seem to provide a very likely candidate for the agent of these perturbations. In this picture, the gas bubbles emitting the subharmonic signal would act primarily as *monitors* of cavitation events, rather than be directly involved in them. This of course is not to say that, under particular conditions (especially in strong cavitation) they would not undergo a collapse, but only that this is not necessary to explain the observed connection between cavitation and subharmonic emission.

The above hypothesis has been based on the assumption that the transient behavior of the first subharmonic models at least qualitatively the characteristics of the oscillations containing a subharmonic component when Eq. 16 is satisfied. This appears to be plausible in view of the fact that, as is easily shown (see, e.g., Ref. 22), the equations determining the amplitude $C_{1/2}$ of the Fourier component at half the driving frequency must in any case possess the solution $C_{1/2}=0$. From the mathematical point of view, therefore, one is faced by a bifurcation problem that can be expected to have similar characteristics in both cases (Ref. 16, Chap. 7). The possibility of a mechanism of this kind is also confirmed by some experiments conducted by Bohn,²³ who observed that under weak cavitation conditions gas bubbles smaller than resonance size can be excited to oscillate at their natural frequency by cavitation shocks. If the sound intensity is increased to strong cavitation conditions,

these bubbles become unstable and break up. This effect, together with the lower transparency to sound of a strongly cavitating liquid, can be responsible for the observed decrease in the subharmonic signal at higher pressure amplitudes.

Clearly, the subharmonic is not the only resonance that could be excited by cavitation shocks. In particular, one might try to correlate the inception of cavitation directly with one or several of the signals corresponding to Eq. 16 for $k \geq 3$.²⁴ Still, the subharmonic does have the great advantage of being in the relatively quiet region below the frequency of the sound field. Over the other possible signals in this region that can be connected with cavitation shocks in the manner described above (notably the second subharmonic), it apparently has the advantage of being more easily excited, so that even the infrequent shocks at the inception of cavitation are sufficient to produce a noticeable emission.

If the hypothesis put forward here is correct, detection of the subharmonic signal should be a useful tool for the determination of cavitation inception for frequencies up to about 1 MHz, because it does not require the presence of bubbles of size much different from those normally present in such cavitation fields. On the other hand, if large bubbles are present (like in the case of gassy liquids⁶ or "prepared" liquids^{7,8}) one could get a subharmonic signal directly from the "subharmonic bubbles" (i.e., those such that $\omega/\omega_0 \sim 2$) without cavitation, since the threshold for their subharmonic excitation may be smaller than that for cavitation.⁷⁻⁹ At frequencies in the megahertz range, the subharmonic bubbles have a radius $R_0 \sim 10^{-3}$ cm (cf. Eq. 6), which is about the order of magnitude of nuclei in freshly drawn tap water (Ref. 1, p. 125). *A priori*, therefore, one could expect a subharmonic signal not to be connected with cavitation. On the other hand, the threshold for emission from the subharmonic bubbles increases with decreasing radius^{9,12} so that the actual behavior of the system will be determined by the competition between the two thresholds. It appears that at this stage the question can only be settled by experiment. The results obtained by de Santis *et al.*⁵ seem to indicate that the connection between subharmonic signal and cavitation is maintained at 1 and 4 MHz, but no results are available for higher frequencies.

IV. OTHER FREQUENCY REGIONS

The system determining the amplitude and phase of the resonant component in the vicinity of the first harmonic ($n=2$) is

$$-4\omega\dot{C} = 4\omega bC + \beta_2 \xi^2 \sin\varphi + b g_3 \xi^2 \cos\varphi, \quad (17a)$$

$$-4\omega C\dot{\varphi} = Q_2 C + g_0 C^3 + \xi^2 \beta_2 \cos\varphi - b \xi^2 g_3 \sin\varphi, \quad (17b)$$

where

$$Q_2 = 4\omega^2 - \omega_0^2 - \xi^2(g_1 - g_2),$$

and the functions β_2 , g_2 , g_3 are defined in Appendix A. The shape of the response curves for the steady-state solution is shown in Figs. 9 and 10 and discussed in Refs. 9 and 12. There it is shown that for low damping or high sound intensity the function $C_0(\omega)$ is triple valued

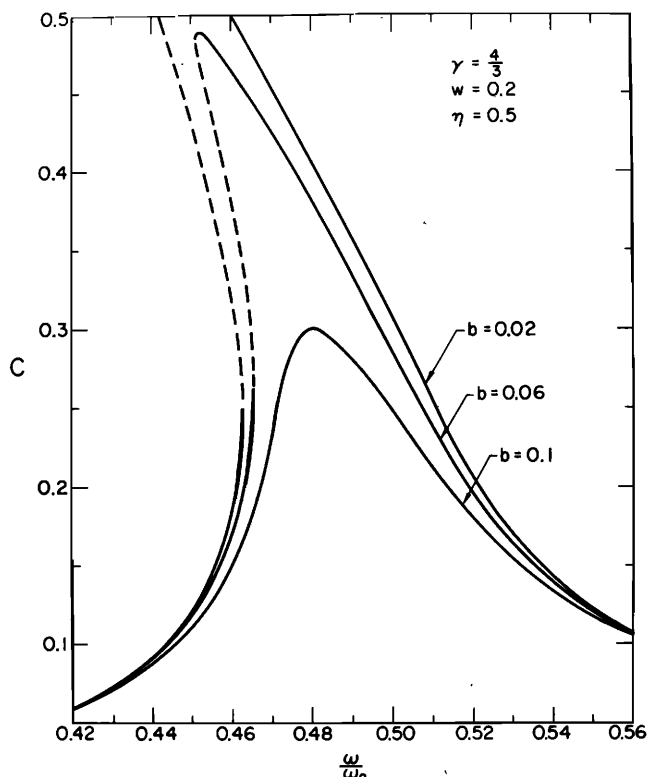


FIG. 9. Amplitude of the steady first harmonic component in a typical case for three values of the damping parameter.

in an interval to the left of $\omega/\omega_0 \sim 1/2$; the intermediate value corresponds to unstable oscillations, while the other two are stable.

In the undamped case the system 17 is Hamiltonian and its solution is given by

$$H = \frac{1}{4}g_0 C^4 + \frac{1}{2}Q_2 C^2 + \beta_2 \xi^3 C \cos \varphi = \text{constant}. \quad (18)$$

The qualitative shape of these curves in the phase plane 12 is shown in Fig. 11 for the case in which there are three singular points. The two stable ones are indicated by large dots, and the unstable one is located at the intersection of the separatrices. As the value of ω/ω_0 is increased towards $1/2$, the two points to the right ($\varphi_0 = 0$) move closer and closer until they merge. If ω/ω_0 is increased still further, only one singular point survives and all trajectories encircle it. The introduction of damping displaces the right singular points downward and towards each other, the left one upward (cf. Fig. 10), and causes all trajectories to approach the steady-state solutions. Essentially, all trajectories starting inside the inner or outer separatrix spiral into the points $|\varphi_0| < (1/2)\pi$ or $|\varphi_0| > (1/2)\pi$, respectively; the trajectories starting outside the domain bounded by the separatrices can end up at either singular point in a fashion similar to that demonstrated in Fig. 5.

The discussion proceeds in a similar manner for the second harmonic and subharmonic regions. For the sake of brevity only the relevant equations will be given here. In the first case $n=3$ and

$$-6\omega\dot{C} = 6\omega b C + g_5 \xi^3 \sin \varphi, \quad (19a)$$

$$-6\omega C \dot{\varphi} = Q_3 C + g_0 C^3 + g_5 \xi^2 \cos \varphi, \quad (19b)$$

where

$$Q_3 = 9\omega^2 - \omega_0^2 - \xi^2(g_1 - g_2);$$

$$H = \frac{1}{4}g_0 C^4 + \frac{1}{2}Q_3 C^2 + g_5 \xi^3 C \cos \varphi. \quad (20)$$

It is evident upon comparison of Eq. 20 with Eq. 18 that the structure of the trajectories in the phase plane will be analogous to the one found in the first harmonic case. Indeed, it is found that the steady response curve determined by Eqs. 19 is qualitatively similar to the one depicted in Fig. 9.^{9,12}

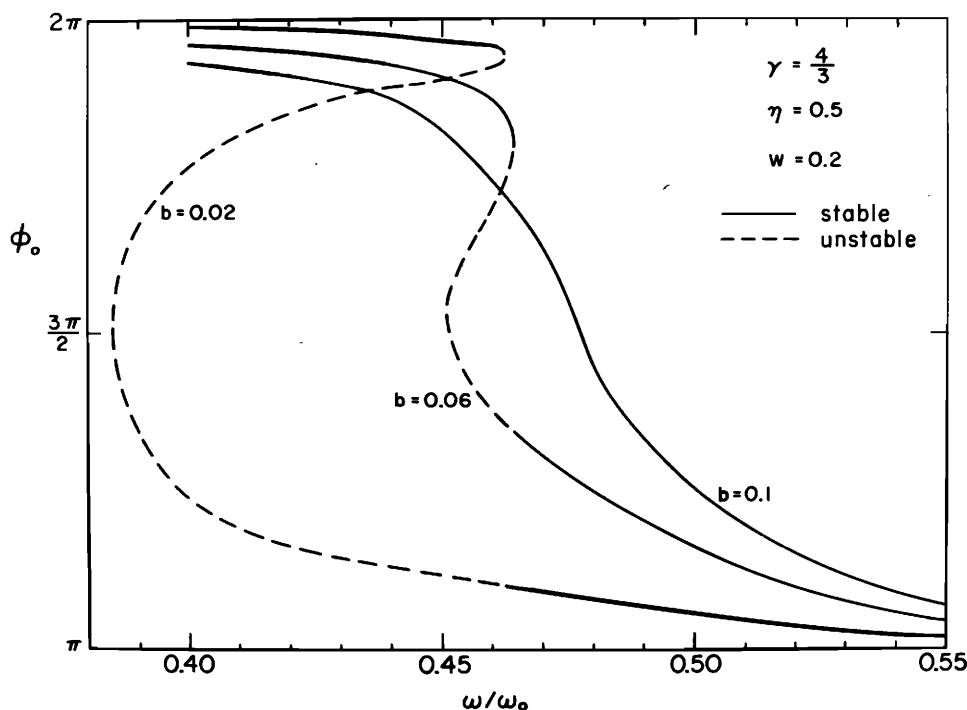


FIG. 10. Phase of the steady first harmonic component, whose amplitude is shown in Fig. 9.

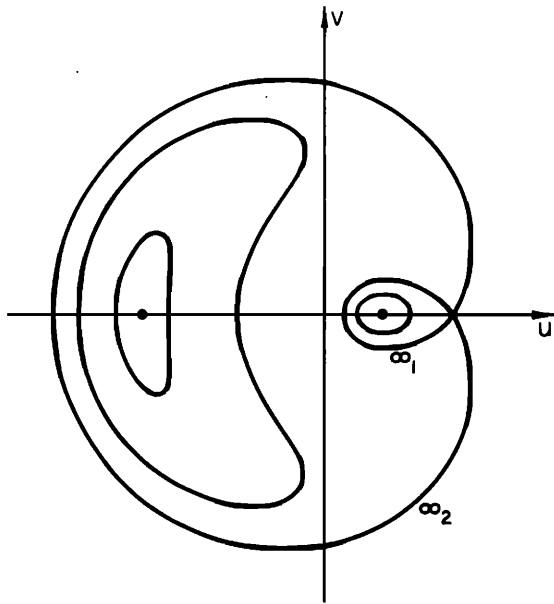


FIG. 11. Qualitative shape of the trajectories determined by Eqs. 17 in the absence of damping. The values of the parameters are such that two stable steady solution exists (large dots). The unstable critical point is at the intersection of the two separatrices on the u axis.

For the second (or $1/3$ order) subharmonic one has

$$-\frac{2}{3}\omega\dot{C} = \frac{2}{3}\omega bC + g_6\xi C^2 \sin 3\varphi, \quad (21a)$$

$$-\frac{2}{3}\omega C\dot{\varphi} = Q_{1/3}C + g_0C^3 + g_6\xi C^2 \cos 3\varphi, \quad (21b)$$

$$Q_{1/3} = \frac{1}{9}\omega^2 - \omega_0^2 - \xi^2(g_1 - g_2),$$

$$H = \frac{1}{4}g_0C^4 + \frac{1}{2}Q_{1/3}C^2 + \frac{1}{3}g_6\xi C^3 \cos 3\varphi.$$

The singular points are now six, three stable and three unstable.^{9,12} In view of the complexity of the phase-plane structure in this case and of the little practical importance of this subharmonic, the properties of these solutions will not be discussed further.

Finally, in the case of the fundamental resonance one has the solution:

$$\begin{aligned} x(\tau) = & C(\tau) \cos \theta + \frac{1}{2}[(4\omega^2 - \omega_0^2)^{-1} \cos(3\omega\tau - \theta) - \omega_0^{-2} \cos \varphi] \\ & \times \xi C(\tau) + \frac{1}{2}[(\alpha_1 - \frac{3}{2}\omega^2)\omega_0^{-2} - (\alpha_1 + \frac{3}{2}\omega^2) \\ & \times (4\omega^2 - \omega_0^2)^{-1} \cos 2\theta] C^2(\tau), \end{aligned}$$

where

$$\theta = \omega\tau + \varphi(\tau).$$

The amplitude C and phase φ are determined by

$$-2\omega\dot{C} = 2\omega bC + (1 - d_3C^2)\xi \sin \varphi + \frac{1}{4}\omega_0^{-2}\xi^2 C \sin 2\varphi, \quad (22a)$$

$$-2\omega C\dot{\varphi} = Q_1C - d_1C^3 + (1 - d_2C^2)\xi \cos \varphi + \frac{1}{4}\omega_0^{-2}\xi^2 C \cos 2\varphi, \quad (22b)$$

$$Q_1 = \omega^2 - \omega_0^2 + \frac{1}{2}\omega_0^{-2}(2\omega^2 - \omega_0^2)(4\omega^2 - \omega_0^2)^{-1}\xi^2.$$

The situation is now complicated by the fact that the system in Eqs. 22 is no longer Hamiltonian. However, both the shape of the steady response curve and the phase-plane structure of the solutions are similar to the ones found in the case of the first and second harmonic.

V. FREE OSCILLATIONS

To analyze the case of free oscillations we set $\xi=0$ in Eq. 5. The equation to be studied becomes then

$$\ddot{x} + \omega_0^2 x = \alpha_1 x^2 - \frac{3}{2}\dot{x}^2 - 2b\dot{x} + \frac{3}{2}x\dot{x}^2 - \alpha_2 x^3 + 4bx\dot{x}.$$

The approximate solution of this equation valid in the presence of damping is

$$x(\tau) = C(\tau) \cos \theta + C^2(\tau)[h_1 - h_2 \cos 2\theta], \quad (23)$$

where

$$C(\tau) = C_0 e^{-b\tau};$$

$$\theta = \omega_0\tau + \varphi_0 - \frac{1}{2}\omega_0 b^{-1}h_3 C_0^2(1 - e^{-2b\tau}), \quad (24)$$

with $C_0 = C(\tau=0)$, $\varphi_0 = \theta(\tau=0)$, and

$$\begin{aligned} h_1 &= \frac{1}{2}\left(\frac{\alpha_1}{\omega_0^2} + \frac{3}{2}\right), \quad h_2 = \frac{1}{6}\left(\frac{\alpha_1}{\omega_0^2} + \frac{3}{2}\right), \\ h_3 &= \frac{1}{4}\left[5\frac{\alpha_1}{\omega_0^2}\left(\frac{1}{3}\frac{\alpha_1}{\omega_0^2} - \frac{1}{2}\right) - \frac{3}{2}\frac{\alpha_2}{\omega_0^2} + \frac{9}{4}\right]. \end{aligned} \quad (25)$$

For large bubbles ($w \sim 0$) these expressions become

$$h_1 = \frac{3}{4}\gamma, \quad h_2 = \frac{1}{2}(\frac{1}{2}\gamma + 1), \quad h_3 = \frac{1}{16}(6\gamma^2 - 3\gamma - 2).$$

If the damping is so small that $4\pi b/\omega_0 \ll 1$, from Eq. 24 one obtains

$$\theta \approx (1 - h_3 C_0^2)\omega_0\tau + \varphi_0 \quad (26)$$

This result exhibits the effect of the nonlinearity on the natural frequency of the system showing that, since $h_3 > 0$, the period of the oscillations increases with their amplitude. The shift in frequency due to damping, being of order b^2 , is obviously absent from Eq. 26, but can be introduced *a posteriori* to obtain the following approximate expression for the nonlinear eigenfrequency of the bubble:

$$\omega_{NL} = [1 - h_3 C_0^2 - \frac{1}{2}(b/\omega_0)^2]\omega_0. \quad (27)$$

The error in this expression is of orders bC_0^2 , b^3 , C_0^3 . Figure 12 presents a plot of ω_{NL}/ω_0 as a function of $C_0 \sim (R_{\max} - R_0)/R_0$ for a bubble of radius $R_0 = 10^{-2}$ cm in water; in order to compare the results with Lauterborn's numerical ones¹⁰ (dashed line in Fig. 12) only viscous damping has been included and $\gamma = 1.33$. It will be noticed that Eq. 27 predicts ω_{NL}/ω_0 within 5% up to C_0

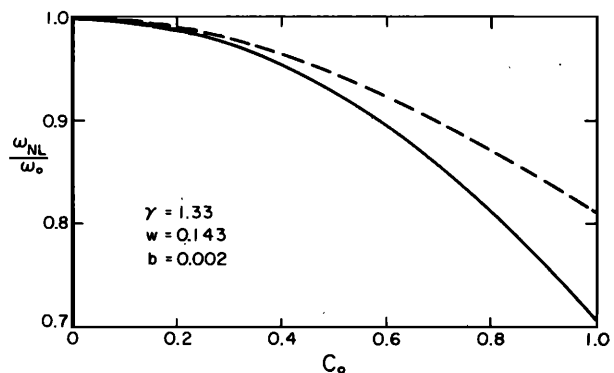


FIG. 12. Comparison between the analytical result for the frequency of nonlinear oscillations, Eq. 27 (full line), and Lauterborn's numerical one (dashed line).

~ 0.5 . As R_0 decreases, h_3 increases so that the range of validity of our results is expected to decrease somewhat. In any event, this agreement gives further reassurance on their accuracy. The logarithmic decrement is obtained as:

$$\Lambda = 2\pi b/\omega_{NL} = (\omega_0/\omega_{NL})\Lambda_0 \quad (28)$$

where $\Lambda_0 = 4\pi\mu/\rho R_0^2\Omega_0$ is the logarithmic decrement of the small amplitude (linear) oscillations. It is obvious from Eq. 27 that Λ is an increasing function of C_0 . The decrease in the logarithmic decrement obtained by Lauterborn for relatively high amplitudes (≥ 0.4) is therefore not reproduced by the present results. The increase in damping for nonlinear oscillations of moderate amplitude appears to be borne out by experiment,²⁶ although no quantitative comparison is possible on the basis of the published data.

The undamped oscillations are also governed by Eq. 23, but now C is a constant and the phase is given by

$$\theta = (1 - h_3 C^2)\omega\tau + \varphi_0.$$

The nonlinear eigenfrequency is therefore seen to be the same as that found above, as it should.

It may be remarked that in the case of free oscillations the Rayleigh-Plesset equation can be written as

$$E(x, \dot{x}) = -4b(1+x)\dot{x}^2,$$

where

$$E(x, \dot{x}) = (1+x)^3\dot{x}^2 + \frac{2}{3}\left[\frac{1}{\gamma-1}(1+x)^{-3(\gamma-1)} + (1-w)(1+x)^3\right] + w(1+x)^2$$

is the total (nondimensional) energy of the system. In the undamped case, then, one obtains the integral of the motion $E(x, \dot{x}) = E_0$ from which x can in principle be determined. For the particular case $\gamma = 4/3$, $w = 0$, $x_0 = x_{\max}$ or x_{\min} , $\dot{x}_0 = 0$ this procedure has recently been followed by Childs.²⁷ In particular, he obtains an analytic expression for the oscillation frequency in terms of elliptic functions.

ACKNOWLEDGMENTS

The author wishes to thank Professor Milton S. Plesset and Professor Thomas K. Caughey for many enlightening discussions concerning the subject of this study.

APPENDIX A

The form of the various functions of ω which appear in the text are given below. The auxiliary quantity D is defined as

$$D = (\omega_0^2 - \omega^2)^{-1}.$$

$$[\omega_0^2 - (n-1)^2\omega^2]c_0(\omega) = D(\alpha_1 - \frac{3}{2}n\omega^2) - \frac{1}{2}, \quad (A1)$$

$$\omega_0^2 c_1(\omega) = \frac{1}{2}D[D(\alpha_1 - \frac{3}{2}\omega^2) - 1], \quad (A2)$$

$$(\omega_0^2 - 4n^2\omega^2)c_2(\omega) = \frac{1}{2}(\alpha_1 + \frac{3}{2}n^2\omega^2), \quad (A3)$$

$$(\omega_0^2 - 4\omega^2)c_3(\omega) = \frac{1}{2}D[D(\alpha_1 + \frac{3}{2}\omega^2) - 1], \quad (A4)$$

$$[\omega_0^2 - (n+1)^2\omega^2]c_4(\omega) = D(\alpha_1 + \frac{3}{2}n\omega^2) - \frac{1}{2}, \quad (A5)$$

$$\omega_0^2 c_5(\omega) = \frac{1}{2}(\alpha_1 - \frac{3}{2}n^2\omega^2), \quad (A6)$$

$$c_6(\omega) = 2\omega D^2. \quad (A7)$$

$$\beta_1(\omega) = \frac{1}{2} - D(\alpha_1 - \frac{3}{2}n\omega^2) \quad (A8)$$

$$\beta_2(\omega) = \frac{1}{2}D[D(\alpha_1 + \frac{3}{2}\omega^2) - 1]. \quad (A9)$$

$$g_0(\omega) = \alpha_1(2c_5 + c_2) + \frac{3}{2}n^2\omega^2(\frac{1}{4} - 2c_2) - \frac{3}{4}\alpha_2, \quad (A10)$$

$$g_1(\omega) = -2\alpha_1 c_1 + c_4\left\{\frac{1}{2} - D\left[\alpha_1 - \frac{3}{2}(n+1)\omega^2\right]\right\} + \frac{3}{2}(\alpha_2 - \frac{1}{2}\omega^2)D^2 - D, \quad (A11)$$

$$g_2(\omega) = c_0\left\{D\left[\alpha_1 + \frac{3}{2}(n-1)\omega^2\right] - \frac{1}{2}\right\}, \quad (A12)$$

$$g_3(\omega) = c_6\left[D(\alpha_1 + \frac{3}{2}\omega^2) - \frac{1}{2}\right] - 2D^2\omega, \quad (A13)$$

$$g_4(\omega) = c_6(\alpha_1 - \frac{3}{2}n\omega^2) + 2(n-1)\omega D, \quad (A14)$$

$$g_5(\omega) = c_3\left[D(\alpha_1 + 3\omega^2) - \frac{1}{2}\right] + \frac{1}{4}[1 - D(\alpha_2 + \frac{3}{2}\omega^2)]D^2, \quad (A15)$$

$$g_6(\omega) = c_0\left[\alpha_1 + \frac{3}{2}n(n-1)\omega^2\right] + c_2\left[D(\alpha_1 - 3n\omega^2) - \frac{1}{2}\right] + \frac{1}{4} + \frac{3}{4}[n(1 - \frac{1}{2}n)\omega^2 - \alpha_2]D. \quad (A16)$$

$$d_1(\omega) = \frac{3}{4}\alpha_2 - \alpha_1\left[\omega_0^{-2}(\alpha_1 - \frac{3}{2}\omega^2) + \frac{1}{2}(\alpha_1 + \frac{3}{2}\omega^2)(\omega_0^2 - 4\omega^2)^{-1}\right] - \frac{3}{2}\omega^2\left[\frac{1}{4} - (\alpha_1 + \frac{3}{2}\omega^2)(\omega_0^2 - 4\omega^2)^{-1}\right], \quad (A17)$$

$$d_2(\omega) = \frac{3}{4}(\alpha_1 - \frac{3}{2}\omega^2)(\omega_0^2 - 4\omega^2)^{-1} + \frac{3}{2}\omega_0^{-2}(\alpha_1 - \frac{1}{2}\omega^2) - \frac{3}{4}, \quad (A18)$$

$$d_3(\omega) = \frac{1}{4}(\alpha_1 - \frac{15}{2}\omega^2)(\omega_0^2 - 4\omega^2)^{-1} + \frac{1}{2}\omega_0^{-2}(\alpha_1 - \frac{3}{2}\omega^2) - \frac{1}{4}. \quad (A19)$$

Finally we give approximate expressions for the functions appearing in the subharmonic region. Letting $\omega = 2\omega_0$ (with $\omega_0^2 = 3\gamma - w$) in Eqs. A8, A10, and A11 one gets

$$\beta_1(2\omega_0) = \frac{1}{8}\omega_0^{-2}(9\gamma^2 - w),$$

$$g_0(2\omega_0) = \frac{1}{8}\omega_0^{-2}[\gamma^2(54\gamma^2 - 27\gamma - 18) + w\gamma(27\gamma^2 - 21\gamma + 18) - \frac{7}{3}w^2],$$

$$g_1(2\omega_0) = \frac{1}{2}\omega_0^{-6}[\gamma^2(\frac{9}{16}\gamma^2 + 9\gamma + 1) - \gamma w(\frac{3}{2}\gamma^2 + \frac{17}{8}\gamma + \frac{11}{8}) + \frac{65}{144}w^2].$$

*On leave of absence from Istituto di Fisica, Università degli Studi, Milano, Italy.

¹H. G. Flynn, *Physical Acoustics*, W. P. Mason, Ed. (Academic, New York, 1964), Vol. 1, Part B, pp. 57-172.

²B. E. Noltingk and E. A. Neppiras, *Proc. Phys. Soc. Lond.* **63B**, 674-685 (1950).

³M. I. Borotnikova and R. I. Soloukhin, *Sov. Phys. Acoust.* **10**, 28-32 (1964).

⁴R. Esche, *Acustica* **2**, 208-218 (1952).

⁵P. de Santis, D. Sette, and F. Wanderlingh, *J. Acoust. Soc. Am.* **42**, 514-516 (1967).

⁶P. W. Vaughan, *J. Sound Vib.* **7**, 236-246 (1968).

⁷E. A. Neppiras, *J. Sound Vib.* **10**, 176-186 (1969).

⁸E. A. Neppiras, *J. Acoust. Soc. Am.* **46**, 587-601 (1969).

⁹A. Prosperetti, *J. Acoust. Soc. Am.* **56**, 878-885 (1974).

¹⁰W. Lauterborn, "Numerical Investigation of Nonlinear Oscillations of Gas Bubbles in Liquids I. Free Oscillations and Frequency Response Curves" (to be published).

¹¹M. S. Plesset, *J. Appl. Mech.* **16**, 277-282 (1949); D. Y. Hsieh, *J. Basic Eng.* **87**, 991-1005 (1965).

¹²A. Prosperetti, "Nonlinear Oscillations of Gas Bubbles in Liquids," Rep. No. 85-62, C.I.T., Div. of Eng. Appl. Sci. (1973).

¹³M. Minnaert, *Philos. Mag.* **16**, 235-248 (1933).

¹⁴R. B. Chapman and M. S. Plesset, *J. Basic Eng.* **93**, 373-376 (1971).

¹⁵N. N. Bogoliubov and N. M. Krylov, *Introduction to Nonlinear Mechanics* (Princeton U.P., Princeton, NJ, 1943); N. N. Bogoliubov and Y. A. Mitropolski, *Asymptotic Methods in the Theory of Nonlinear Oscillations* (Hindustan, New Delhi, 1961).

- ¹⁶N. Minorski, *Nonlinear Oscillations* (Van Nostrand, Princeton, NJ, 1962), Chap. 14 and 15.
- ¹⁷The values of C and φ at $\tau=0$ needed for the integration of system 9 are obtained from Eq. 7 and its time derivative as a function of $x(\tau=0)$ and $\dot{x}(\tau=0)$.
- ¹⁸The minimum value of H corresponding to real orbits is $H_{\min} = -(\beta_1 \xi - Q_{1/2})^2/g_0$; when $H=H_{\min}$ the trajectories degenerate into the nonzero stable singular points. For $H_{\min} \leq H < H_{\text{cr}}$, with $H_{\text{cr}} = -(\beta_1 \xi + Q_{1/2})^2/g_0$, one has the "subharmonic" orbits. The value $H=H_{\text{cr}}$ corresponds to the two separatrices, and for $H_{\text{cr}} < H < 0$ one has both "harmonic" and outer orbits. Finally, for $H=0$ the harmonic orbit degenerates into the point $C=0$, and for positive values of H only the outer orbits are present. For additional details, see Ref. 12.
- ¹⁹The period on a separatrix is always infinite, since in the vicinity of an equilibrium point the derivatives are vanishingly small. This may be the reason for some numerical difficulties reported by Eller in Ref. 20.
- ²⁰A. I. Eller, *J. Acoust. Soc. Am.* 55, 871-873 (1974).
- ²¹Lauterborn states in Ref. 10 that most of his computations were started from the equilibrium conditions $R=R_0$, $dR/dt=0$.
- ²²A. Prosperetti, "Subharmonics and Ultraharmonics in the Forced Oscillations of Nonlinear Systems," *Am. J. Phys.* (in press).
- ²³L. Bohn, *Acustica* 7, 201-216 (1957).
- ²⁴Most likely, bubbles corresponding to a low value of k , such as $k=3, 4$ and possibly 5 would be more easily excited. Indeed the harmonic at $\omega/\omega_0=3/2$ appears to be present in all the spectra published by Esche (Ref. 4) and by K. Negeshi [*J. Phys. Soc. Jpn.* 16, 1450 (1961)] with an intensity very near to that of the subharmonic. The numerical results of Lauterborn (Figs. 15 and 16 of Ref. 10) show that the amplitude of the first subharmonic is not necessarily smaller than that of the "primary" fractional harmonic, Eq. 16.
- ²⁵W. Lauterborn, *Acustica* 23, 73-81 (1970).
- ²⁶H. G. Koger and G. Houghton, *J. Acoust. Soc. Am.* 43, 571-575 (1968).
- ²⁷D. R. Childs, *Int. J. Non-Linear Mech.* 8, 371-379 (1973).